A Heterobimetallic Vanadium−Manganese Complex as a Model for the Structural Dynamics in Oxo-Bridged Metal Dimers

Norman S. Dean,[†] Jennifer K. Cooper,[†] Roman S. Czernuszewicz,[‡] David Ji,[‡] and Carl J. Carrano*,[†]

Departments of Chemistry, Southwest Texas State University, San Marcos, Texas 78666, and University of Houston, Houston, Texas 77204

Received December 30, 1996[⊗]

The heterobimetallic complex **1**, [LV(μ-O)(μ-OAc)$_2$MnL] (where L = hydridotris(pyrazolyl)borate), has been synthesized and characterized. X-ray crystal structural analysis of **1** gave the following parameters: $C_{24}H_{29}B_2N_{13}O_5$-VMn, $Cmc2_1$, a = 13.364(2) Å, b = 17.383(3) Å, c = 14.132(3) Å, Z = 4, V = 3289.9(16) Å^3. An analysis of the structure, optical and resonance Raman spectroscopies, and magnetic measurements indicates that a V^{IV}═O···Mn^{II} valence formulation is the best description of the oxo-bridged core in **1**, although other resonance forms must also contribute.

Introduction

Oxo-bridged units have been found to be an important structural motif in the chemistry of first-row transition metals, particularly manganese,[1] iron,[2] and vanadium.[3] These units are also ubiquitous in biological systems with a growing body of metalloproteins and metalloenzymes having been isolated which incorporate μ-oxo-bridged motifs at their active sites to carry out a wide range of functions. For example, a μ-oxo-bridged dimetal unit has been structurally characterized by single-crystal X-ray crystallography in iron-containing hemerythrins[4] and ribonucleotide reductase[5] while the involvement of μ-oxo-bridged as well as di-μ-oxo-bridged dinuclear units has been implicated in manganese-containing catalases from spectroscopic probes of structure.[6] The tetramanganese water oxidase enzyme of the green plant photosystem II is also believed to contain an oxo-bridged active site,[7,8] and involvement of a V−O−V dimer in the biology of vanadium is suspected on the basis of spectrochemical evidence.[9]

These oxo-bridged active sites also display unique electronic and magnetochemical properties stemming from the superexchange pathways mediated by the bridging oxide, such as strong O → M charge-transfer (CT) transitions in the visible region and varying degrees of magnetic coupling. The CT and magnetic interactions that take place through the agency of an oxo bridge reflect the overlap between metal and oxygen orbitals and, hence, depend on the extent of metal−oxygen interactions. Subtle changes in the M−O interactions as a function of the electronic configuration of the metal atom can thus lead to variable, and sometimes different, ground and excited state electronic properties.

Of the various known structural types of oxo-bridged metal dimers, perhaps the best studied are the bent cobridged structures represented by [$M_2O(O_2CCH_3)_2(HB(pz)_3)_2$] and their TACN analogs. The molecular structures of complexes with iron(III), manganese(III), and vanadium(III) have all been solved and their M−O−M vibrational signatures elucidated by a number of resonance Raman studies.[10−13] In particular we have extensively investigated the physicochemical properties of V−O−V dimers and compared them with the analogous Fe and Mn complexes.[13] Using resonance Raman spectroscopy and calculations based on a triatomic harmonic oscillator approximation it was shown that decreasing patterns of interaction constants from Fe(III) to V(III) implicated an increased dynamic stabilization of an excited state that is increasingly asymmetrical due to differential electronic interaction of the oxygen with the two metal ions of the M−O−M core. In this work we describe a stable ground state structure that resembles the excited state geometry implicated by the previous work.

Experimental Section

Materials. All synthetic procedures were carried out under an atmosphere of pure dry argon or nitrogen by utilizing standard Schlenk techniques. Subsequent workup was carried out in air unless otherwise noted. Solvents were distilled under nitrogen from the appropriate drying agents (CaH_2 or Na/benzophenone). DMF was Burdick and Jackson "distilled in glass" grade and was used as received following storage under nitrogen. All other materials were reagent grade and used as received. Potassium hydridotris(pyrazolyl)borate was synthesized according to the reported method,[14] as was [$HB(pz)_3$]VCl_2DMF.[15]

Synthesis. [$HB(pz)_3V(\mu$-O)(μ-$OAc)_2MnHB(pz)_3$] (1). To a solution of [$HB(pz)_3$]VCl_2DMF (0.82 g, 2.0 mmol) dissolved in 40−50 mL of CH_3CN was added, with constant stirring, 0.49 g of $Mn(OAc)_2$ (2.0 mmol). To the resulting deep reddish brown solution was added an equimolar quantity of $KHB(pz)_3$ (0.50 g, 2.0 mmol). The solution

[†] Southwest Texas State University.
[‡] University of Houston.
[⊗] Abstract published in *Advance ACS Abstracts,* June 1, 1997.

(1) Wieghardt, K. *Angew. Chem., Int. Ed. Engl.* **1989**, *28*, 1153.
(2) Lippard, S. J. *Angew. Chem., Int. Ed. Engl.* **1988**, *27*, 349.
(3) Rehder, D. *Angew. Chem., Int. Ed. Engl.* **1990**, *30*, 148.
(4) Stenkamp, R. E.; Sieker, L. C.; Jensen, L. H.; McCallum, J. D.; Sanders-Loehr, *J. Proc. Natl. Acad. Sci. U.S.A.* **1985**, *82*, 713.
(5) Nordlund, P.; Eklund, H. J. *J. Mol. Biol.* **1993**, *232*, 123.
(6) Penner-Hahn, J. E. In *Manganese Redox Enzymes*; Pecoraro, V. L., Ed.; VCH Publishers: New York, 1992; p 29.
(7) Dismukes, G. C. *Photochem. Photobiol.* **1986**, *43*, 99.
(8) Brudvig, G. W.; Crabtree, R. H. *Prog. Inorg. Chem.* **1989**, *37*, 99.
(9) Anderson, D. H.; Swinehart, J. H. *Comp. Biochem. Physiol.* **1991**, *99a*, 585.
(10) Armstrong, W. H.; Spool, A.; Papaefthymiou, G. C.; Frankel, R. B.; Lippard, S. J. *J. Am. Chem. Soc.* **1984**, *106*, 3653.
(11) Czernuszewicz, R. S.; Sheats, J. E.; Spiro, T. G. *Inorg. Chem.* **1987**, *26*, 2063.
(12) Sheats, J. E.; Czernuszewicz, R. S.; Dismukes, G. C.; Rheingold, A. L.; Petrouleas, V.; Stubbe, J.; Armstrong, W. H.; Beer, R. H.; Lippard, S. J. *J. Am. Chem. Soc.* **1987**, *109*, 1435.
(13) Bond, M. R.; Czernuszewicz, R. S.; Dave, B. C.; Mohan, M.; Verastque, R.; Carrano, C. J. *Inorg. Chem.* **1995**, *34*, 5857.
(14) Trofimenko, S. *J. Am. Chem. Soc.* **1967**, *89*, 3170.
(15) Mohan, M.; Holmes, S. M.; Butcher, R. J.; Jasinski, J. P.; Carrano, C. J. *Inorg. Chem.* **1992**, *31*, 2029.

S0020-1669(96)01533-9 CCC: $14.00

Table 1. Crystallographic Data and Data Collection Parameters for **1**

param	**1**
formula	$C_{24}H_{29}B_2MnN_{13}O_5V$
space group	$Cmc2_1$
temp, K	298
a, Å	13.364(2)
b, Å	17.383(3)
c, Å	14.132(3)
V, Å^3	3282.9(16)
ρ_{calc}, g cm^{-3}	1.431
Z	4
fw	707.1
cryst size, mm	0.8 × 0.8 × 0.8
μ, cm^{-1}	7.24
radiation	Mo Kα
scan type	$\theta-2\theta$
data collection range, deg	3.5−45
R_{merge}, %	2.24
no. of unique data	1292
no. of obs data, $F > 4.0s(F)$	1262
data:param ratio	5.4:1
transm	0.8417/0.9051
R,[a] %	3.16
R_w,[a] %	4.26
max diff peak, e/Å^3	0.30
Δ/σ(mean)	0.004

[a] Quantity minimized $\omega w(F_o - F_c)^2$, $R = \Sigma|F_o - F_c|/\omega F_o$. $R_w = (\omega w(F_o - F_c)^2/\Sigma(wF_o)^2)^{1/2}$.

was heated to dissolve the potassium hydridotris(pyrazolyl)borate, and the dark cloudy green reaction mixture was filtered. Upon standing overnight, crystals of **1** suitable for X-ray analysis were isolated by filtration and air-dried. Yield: 0.44 g, 33%. Anal. Calcd for **1**·CH_3-CN: C, 40.77; H, 4.13; N, 25.75. Found: C, 40.73; H, 4.13; N, 25.49. IR (cm^{-1}) 2518, 1594, 1502, 1398, 1300, 1207, 1109, 1049, 979, 930, 772, 717, 537.

Physical Methods. Preliminary determinations of magnetic susceptibilities were made at room temperature using a Johnson-Mathey magnetic susceptibility balance while variable temperature measurements were performed as previously described over the range 2−300 K employing a SQUID magnetometer.[16] UV−vis spectra were recorded on an HP8452A diode array spectrophotometer. Resonance Raman spectra were recorded and analyzed as previously reported.[17−19] Elemental analyses were performed by Desert Analytical Services.

X-ray Crystallography. Crystals of **1** were sealed in a Lindeman glass capillary and mounted on a Siemens P4 diffractometer. Unit cell constants were determined by least squares refinement of the angular settings of 20 well-centered relatively high angle reflections. Systematic absences did not unambiguously determine the space group, but the $|E^*E-1|$ statistics clearly favored a noncentric group, of which $Cmc2_1$ was the most common. Successful solution and refinement, achieved using the SHELXTL-PLUS crystallography software from Siemens,[20] validated this choice. Positions for all the non-hydrogen atoms of the dimer were evident on the *E*-map with the V, Mn, μ-O, B, and two pyrazole rings sitting on a mirror plane. An acetonitrile of crystallization also became evident on subsequent electron density difference maps. Hydrogen atoms were calculated and given isotropic thermal parameters fixed at 0.08 Å^2. Pertinent parameters regarding crystal data, data collection, and structure solution and refinement can be found in Table 1, with selected bond lengths and angles in Table 2.

Table 2. Bond Lengths (Å)

Mn(1)−N(8)	2.209(5)	Mn(1)−O(3)	2.120(4)
Mn(1)−O(2)	2.201(5)	Mn(1)−N(7)	2.234(5)
Mn(1)−N(8A)	2.209(5)	Mn(1)−O(3A)	2.120(4)
V(1)−O(2)	1.667(6)	V(1)−O(1)	2.008(4)
V(1)−N(3)	2.124(4)	V(1)−N(2)	2.242(6)
V(1)−O(1A)	2.008(4)	V(1)−N(3A)	2.124(4)

N(8)−Mn(1)−O(3)	89.2(2)	N(8)−Mn(1)−O(2)	91.2(1)
O(3)−Mn(1)−O(2)	87.2(1)	N(8)−Mn(1)−N(7)	83.2(1)
O(3)−Mn(1)−N(7)	97.9(1)	O(2)−Mn(1)−N(7)	172.4(2)
N(8)−Mn(1)−N(8A)	85.9(2)	O(3)−Mn(1)−N(8A)	174.9(2)
O(2)−Mn(1)−N(8A)	91.2(1)	N(7)−Mn(1)−N(8A)	83.2(1)
N(8)−Mn(1)−O(3A)	174.9(2)	O(3)−Mn(1)−O(3A)	95.5(2)
O(2)−Mn(1)−O(3A)	87.2(1)	N(7)−Mn(1)−O(3A)	97.9(1)
N(8A)−Mn(1)−O(3A)	89.2(2)	O(2)−V(1)−O(1)	97.9(2)
O(2)−V(1)−N(3)	96.6(2)	O(1)−V(1)−N(3)	90.6(1)
O(2)−V(1)−N(2)	177.4(2)	O(1)−V(1)−N(2)	84.0(2)
N(3)−V(1)−N(2)	81.5(2)	O(2)−V(1)−O(1A)	97.9(2)
O(1)−V(1)−O(1A)	89.7(2)	N(3)−V(1)−O(1A)	165.3(2)
N(2)−V(1)−O(1A)	84.0(2)	O(2)−V(1)−N(3A)	96.6(2)
O(1)−V(1)−N(3A)	165.3(2)	N(3)−V(1)−N(3A)	85.5(2)
N(2)−V(1)−N(3A)	81.5(2)	O(1A)−V(1)−N(3A)	90.6(1)

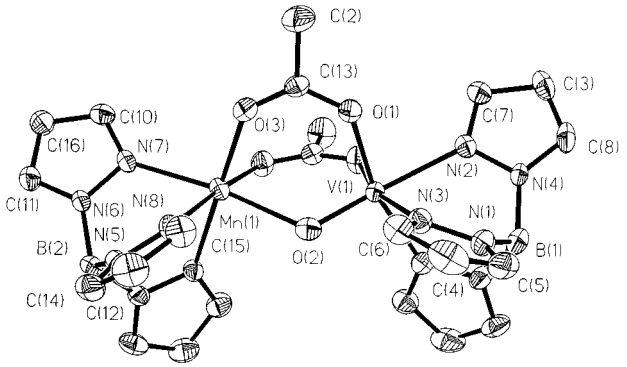

Figure 1. ORTEP diagram with 30% probability ellipsoids for **1** showing complete atomic labeling.

Results

Synthesis. The $LVCl_2DMF/Mn(OAc)_2$ reaction system was originally investigated by us as a route for preparing heterometallic acetate-bridged trinuclear species analogous to the phosphate-bridged species previously reported.[21,22] However, upon addition of 0.5 equiv of $Mn(OAc)_2$ to $LVCl_2DMF$ followed by two sequential additions of sodium acetate, an orange brown solution was obtained which yielded a small crop of **1** upon evaporation to dryness. On the basis of analysis of the product, it was clear that there was insufficient tris(pyrazolyl)borate in the reaction mixture to produce **1** in good yield. This suggested the modification used in the "rational" synthesis reported here which produced **1**, although still only in fair yield. Encouraged by this initial success we attempted to produce analogous V−O−M heterobimetallic complexes where M = Co, Ni, and Fe. Unfortunately in all cases the only crystallographically characterizable product was the corresponding L_2M "sandwich" complex. Likewise, attempts to synthesize the mixed-ligand complex, $[HB(pz)_3]V(\mu\text{-O})(\mu\text{-OAc})_2Mn[HB(3,5\text{-Mepz})_3]$, also met with failure.

Description of Structure. The structure of **1**, shown in Figure 1 with the atom-labeling scheme, displays a number of notable features with respect to the corresponding M(III) homometallic dimers of relevance to the question of the

(16) O'Connor, C. J. *Prog. Inorg. Chem.* **1982**, *29*, 203.
(17) Czernuszewicz, R. S. *Appl. Spectrosc.* **1986**, *40*, 571−573.
(18) Czernuszewicz, R. S.; Johnson, M. K. *Appl. Spectrosc.* **1983**, *37*, 297−299.
(19) Czernuszewicz, R. S. In *Methods in Molecular Biology*; Jones, C., Mulloy, B.,Thomas, A. H., Eds.; Humana Press: Totawa, NJ, 1993, Vol. 17, pp 345−374.
(20) Sheldrick, G. M. *SHELXTL-PC*, Version 4.1; Siemens X-Ray Analytical Instruments, Inc.: Madison, WI, 1989. Scattering Factors from the following: *International Tables for X-Ray Crystallography*; Ibers, J., Hamilton, W., Eds.; Kynoch: Birmingham, U.K., 1974; Vol. IV.
(21) Dean, N. S.; Mokry, L. M.; Bond, M. R.; O'Connor, C. J.; Carrano, C. J. *Inorg. Chem.* **1996**, *35*, 3541.
(22) Dean, N. S.; Mokry, L. M.; Mohan, M.; Bond, M. R.; O'Connor, C. J.; Otieno, T.; Sportalian, K.; Carrano, C. J. *Inorg. Chem.* **1997**, *36*, 1424.

Table 3. Observed Infrared and Raman Spectral Bands (cm^{-1}) and Proposed Assignments for $[VOMn(O_2CCH_3)_2(HB(pz)_3)_2]$ (**1**)

IR[a]	RR[b]	assignment[c]
	287 sh	ν(M−N)$_{pz}$
	304 (11)[d]	ν(Mn−O)$_{oxo}$
353 sh	354	ν(M−O_2CR)
387	387 sh	ν(M−O_2CR)
542 br	542	L
621	619 w	L
661	661	δ(O−C−O)
665	664 sh	δ(O−C−O)
719 s	717 w	
725 sh		
761 s	760 vw	
779 sh		L
793	792 vw	
853 vw, br	851 w, br	
885 w, br		
926 sh (36)	925 vs (37)	ν(V=O)$_{oxo}$
932 m	931 sh	
943 sh	941 sh	
975	974 w	
988 sh	982 sh	
1022 sh	1017 br	
1050 s	1048 vw	
1072 sh	1072 w	
1088 sh	1089 sh	L
1095 w	1093	
1116 s	1115 w	
1192 sh	1190 sh	
1214 s	1216	
1304 s	1302	
1310 s	1309	
1344	1345 vw	
1392	1391	
1405 s	1404 sh	ν_s(O−C−O)
1422 sh	1425	L
1593 s	1594 m, br	ν_{as}(O−C−O)
	1842 (74)	2ν(V=O)$_{oxo}$[e]
2475		ν(B−H)

[a] IR spectra in KBr pellet. [b] Resonance Raman (RR) in KCl pellet kept at liquid N_2 temperature. Symbols: s, strong; m, medium; w, weak, sh, shoulder; br, broad. [c] ν = stretch, δ = deformation, ν_s = symmetric stretch, ν_{as} = asymmetric stretch, L = assigned as vibration of $HB(pz)_3$. [d] Numbers in parentheses indicate the μ-^{18}O → μ-^{16}O isotopic shift upon exchange with $H_2{}^{18}O$. [e] Overtone.

oxidation assignment between the two metals. Most prominent among these is the decided asymmetry in the V−O−Mn bond lengths, *i.e.*, 1.667 Å for the former and 2.201 Å for the latter. The V−O bond is considerably shorter (0.11 Å) than that seen in the analogous divanadium(III) complex and is almost in the range seen for V(IV) vanadyl oxo groups (1.59−1.62 Å) while the Mn−O is some 0.42 Å longer than that seen in the Mn(III) dimer.[12] Thus the structure is more consistent with a V^{IV}═O···Mn^{II} formulation than the alternative V^{III}−O−Mn^{III} one. Wieghardt and co-workers have reported a formally Ru^{II}−O−V^{IV} dimer which shows the same asymmetry.[23] Also consistent with the IV−II formulation is the evident "trans" effect seen around the vanadium, with the V−N bond trans to the bridging oxo group 0.1 Å longer than the two cis V−N interactions. This result is the expected one for a V(IV) oxo center, as is the 0.26 Å displacement of the vanadium from the mean equatorial plane toward the bridging oxygen. The V−O−Mn angle of 123° is 10° less than that found in the all-vanadium dimer but nearly the same as that found in all other metallodimers of this class. Finally, the V···Mn distance of 3.412 Å is considerably longer than that found in either homometallic dimer but consistent with the V^{IV}═O···Mn^{II} assignment.

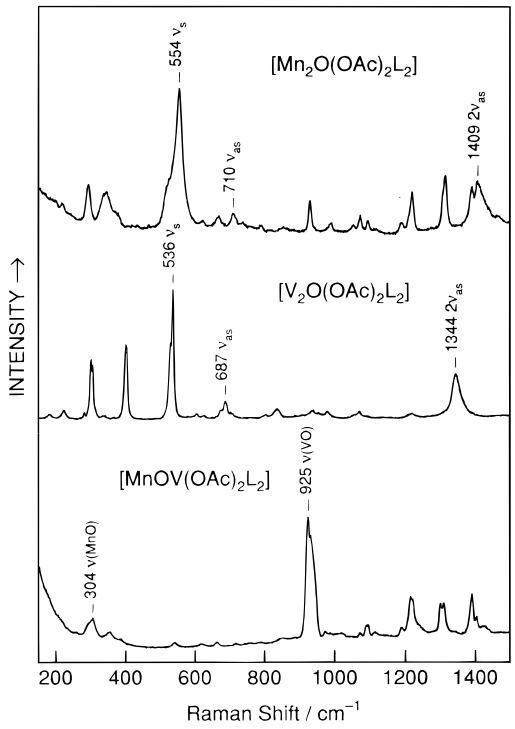

Figure 2. Resonance Raman spectra of **1** (bottom), **2** (middle), and **3** (top). All spectra were obtained via backscattering in KCl pellets at room temperature (**2** and **3**) or 77 K (**1**) by using 406.7 nm (**3**) and 676.4 nm (**2**) Kr^+ and 457.9 nm (**1**) Ar^+ ion laser excitations (200 mW) and 5 cm^{-1} slit widths.

Infrared and Resonance Raman Spectroscopy. Table 3 summarizes the principal infrared and resonance Raman vibrational frequencies and proposed assignments for **1**. Conspicuous features in the infrared spectrum are the pyrazolylborate ligand B−H stretching band at 2475 cm^{-1}, the broad, intense ν_s(OCO) and ν_{as}(OCO) stretching bands at 1405 and 1593 cm^{-1}, respectively, for the carboxylato bridges, and a number of sharp, intense peaks between 600 and 1500 cm^{-1} due to the pyrazolyl ring vibrations.[10−13] A broad, multicomponent band of medium intensity is centered at ∼930 cm^{-1}. One of its components occurs at ∼926 cm^{-1} and is assigned to the stretching vibration of the V−O−Mn bridge on the basis of the appearance of a dominant, polarized peak at 925 cm^{-1} in the resonance Raman spectra of **1** in both the solid state (Figure 2) and solution (Figure 3) when excited with blue-green Ar^+ ion laser lines. As shown in Figure 3 for **1** in $CHCl_3$ solution and with a 457.9 nm excitation wavelength, this band shifts to 889 cm^{-1} with ^{18}O exchange in the bridge, confirming its assignment to the vibrational mode involving a motion of an oxo group. Also evident is a peak at 1842 cm^{-1}, which can be assigned as the first overtone of the 925 cm^{-1} fundamental, and which shifts to 1768 cm^{-1} upon μ-^{18}O exchange.

The symmetric (ν_s) and asymmetric (ν_{as}) V−O−V bridge stretches in the homometallic dimer, $[V_2O(OAc)_2(HB(pz)_3)_2]$ (**2**), occur at 536 (strong) and 687 cm^{-1} (weak), respectively (Figure 2, middle),[13] while typical V═O stretching vibrations occur in the 1010−880 cm^{-1} range.[24,25] Also characteristic for dimer **2** is a resonance Raman band of medium intensity at 1344 cm^{-1} assigned to 2ν_{as}(VOV).[13] The analogous ν_s(MnOMn), ν_{as}(MnOMn), and 2ν_{as}(MnOMn) vibrations in the resonance Raman spectrum of $[Mn_2O(OAc)_2(HB(pz)_3)_2]$ (**3**) are located

(23) Hotzelmann, R.; Wieghardt, K.; Floerke, U.; Haupt, H. J. *Angew. Chem., Int. Ed. Engl.* **1990**, *29*, 645.

(24) Nakamoto, K. *Infrared and Raman Spectra of Inorganic and Coordination Compounds*, 4th ed.; Wiley: New York, 1986.

(25) Czernuszewicz, R. S.; Nakamoto, K.; Okawa, H.; Kida, S. *Inorg. Chim. Acta* **1978**, *27*, L101−L102.

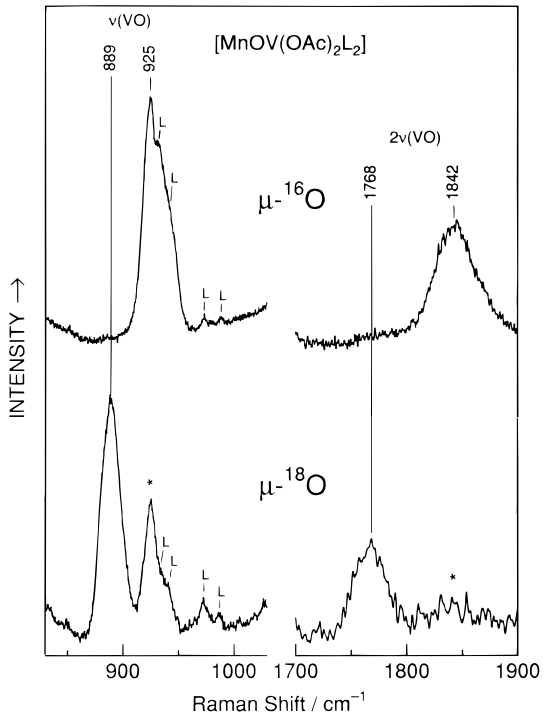

Figure 3. Room-temperature resonance Raman spectra of **1** in $CHCl_3$ and its μ-^{18}O analog obtained via frontscattering from a spinning NMR tube by using 457.9 nm Ar^+ ion laser excitation (200 mW) and 6 cm^{-1} slit widths. "L" marks bands associated with internal modes of $HB(pz)_3^-$ ligands. An asterisk marks bands due to incomplete $^{18}O \rightarrow {}^{16}O$ exchange.

at 554, 710, and 1409 cm^{-1}, respectively (Figure 2, top).[12] Hence, on the basis of its energy and sensitivity to isotopic oxygen substitution, we assign the 925 cm^{-1} peak of **1** to a V═O···Mn stretching vibration which is almost pure V═O in character. Indeed, using a two-atom vibrational model without considering the Mn contribution, the 925 cm^{-1} band is expected to downshift to 885 cm^{-1} upon ^{18}O exchange, which compares well with that observed (889 cm^{-1}). Only one other oxygen sensitive peak is observed in the resonance Raman spectra of **1**, which is at 304 cm^{-1} (Figure 2, bottom) and shifts to 294 cm^{-1} when ^{18}O is substituted in the V−O−Mn bridge (not shown). The same simple two-atom calculation as used previously, this time with the mass contribution of the vanadium being ignored, predicts that the band at 304 cm^{-1} should be downshifted to 291 cm^{-1} for a pure Mn−O stretch. This again compares well with the observed shift, confirming the assignment. These results indicate that, unlike symmetric M−O−M bridges in homometallic dimers **2** and **3**, the V−O−Mn bridge in **1** represents an uncoupled triatomic oscillator due to the large difference in force constants for the V═O and Mn−O bonds, in agreement with the X-ray data.

Optical Spectroscopy. The spectrum of **1** is shown in Figure 4. It does not at all resemble the V(III) homonuclear dimer but has similarities to the Mn(III) analog.[12] The major feature of the spectrum is the broad envelope centered at about 400 nm which clearly consists of at least three overlapping bands. Also evident is a very weak band centered above 820 nm which may be a characteristic d−d band of the V^{IV}═O unit. The magnitudes of the extinction coefficients (399 M^{-1} cm^{-1} at 392 nm and 311 M^{-1} cm^{-1} at 430 nm) are consistent with either d−d bands of the Mn(II) which, although formally spin forbidden, have gained intensity due to the exchange interaction or with charge transfer transitions of the V−O−Mn core. The importance of this latter mechanism is demonstrated by Figure 4, which compares the excitation profile (EP) for the 925 cm^{-1}

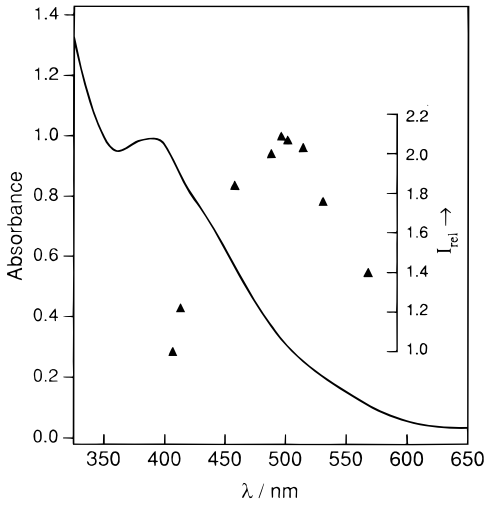

Figure 4. Relative Raman intensity (I_{rel}) profile for the ν(V═O··· Mn) stretching mode at 925 cm^{-1} of crystalline **1**, superimposed on its electronic spectrum in acetonitrile. Raman band intensities were determined relative to the 984 cm^{-1} $\nu_1(SO_4^{2-})$ band and normalized to the intensity at the 406.7 nm excitation wavelength.

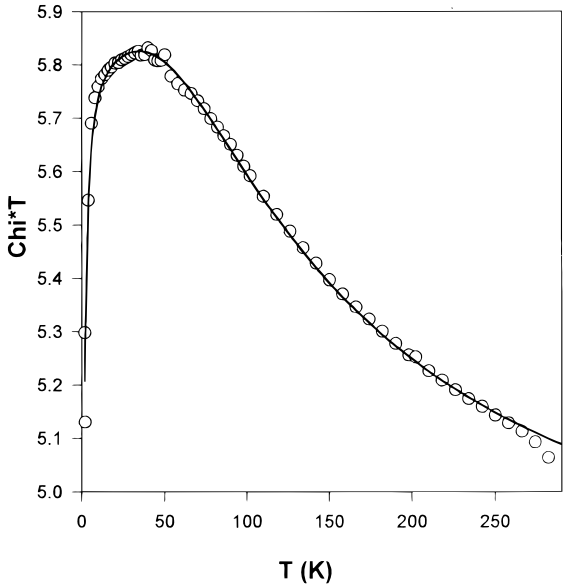

Figure 5. Plot of χT vs T for **1** over the range 2−300 K. The open circles are the data points, and the curve was generated by fits to the model described in the text.

ν(V═O···Mn) Raman band, measured relative to the 984 cm^{-1} ν_1 band of SO_4^{2-} present as an internal standard, with the absorption spectrum of **1**. A well-defined maximum is seen in the EP, at ∼500 nm, indicating an underlying μ-O → V(IV) charge-transfer transition in the visible electronic spectrum.

Magnetism. The magnetic susceptibility of **1** was measured over the range 2−300 K. At room temperature χT has a value somewhat above the uncoupled limit for a noninteracting $S = {}^1/_2$ and $S = {}^5/_2$ dimer but well above that expected for the equivalent $S = 1$ and $S = 2$ description. As the temperature is lowered, χT increases monotonically (Figure 5), reaching at peak near 50 K before falling again below this temperature. This behavior is indicative of moderate ferromagnetic coupling between the metal centers with a weak antiferromagnetic *interdimer* interaction. The interaction between a V(IV) and a Mn(II) gives rise to $S = 2$ and $S = 3$ pair states while that between a V(III) and a Mn(III) gives $S = 1$, $S = 2$, and $S = 3$ states. Not surprisingly that data could be adequately fitted employing either oxidation state formalism using the Heisenberg−Dirac−VanVleck Hamiltonian with an average g value

and a molecular field correction. The fit (Figure 5) for the former description was, however, slightly better than for the latter and gave parameters $J = +22.8$ cm^{-1}, $g = 1.979$, $zJ' = -0.03$ cm^{-1}. The integral spin $S = 3$ ground state implied by this fit is consistent with the lack of an observable EPR spectrum between 298 and 77 K.

Discussion

The present complex complements those studied in previous work and allows a more detailed examination of the bonding and spectroscopic properties of bent M−O−M units. Specifically one of the following resonance structures may represent the bonding in the M−O−M unit.

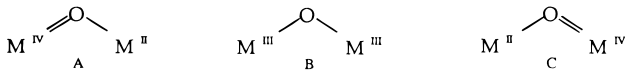

In a homometallic complex, forms A and C are equivalent, while they are different in a heterobimetallic species. In the specific case of the V−O−Mn dimer, they represent the V^{IV}═O···Mn^{II}, V^{III}−O−Mn^{III}, and V^{II}···O═Mn^{IV} formulations. On the basis of our chemical intuition the latter formulation is unlikely to contribute significantly, containing as it does both a strong oxidant in Mn(IV) and a strong reductant in V(II). From the structure of **1** it is clear that form A must be the dominant one. Nevertheless the magnetism and the optical and resonance Raman spectroscopy all indicate that form B probably also contributes.

The ferromagnetic coupling seen in the magnetic behavior of **1** is easily rationalized in terms of a number of models but perhaps most easily with respect to the so-called "crossed interactions" based on the Goodenough−Kanamori rules.[26,27] It is clear that the primary pathway for interaction between the metal centers will be based on superexchange through the bridging oxo group. The acetates are expected to contribute very little to the overall effect. The dominant symmetry-allowed overlaps have been identified as (d_{z^2}|p|d_{z^2}), (d_{yz}|p|d_{yz}), and (d_{xz}|p|d_{z^2}).[27] Since all the allowed interactions are ferromagnetic in nature the overall coupling is ferromagnetic despite the fact that such couplings are generally weaker than antiferromagnetic ones. The magnitude of the coupling seen in **1** is slightly greater than that in the Mn^{III}−O−Mn^{III}, but much less than that in the V^{III}−O−V^{III}, homometallic dimers. The increase in coupling for **1** with respect to the former can be rationalized by the absence of the AFM pathway which is available in the all-Mn dimer,[27] while the decrease from the divanadium system has two possible origins. First, the increasing M−M distance caused by the long Mn−O bond is expected to attenuate the magnitude of the coupling whether it be FM or AFM in nature. Secondly, as the M−O−M angle decreases from 180° toward 120°, the interaction between the metals is expected to become less ferromagnetic as the gain in orbital energy obtained through spin pairing exceeds the spin-pairing energy itself.[13]

The optical spectrum of **1** is noteworthy in that it derives at least partly from oxo to metal charge transfer within the M−O−M unit as confirmed by resonance Raman spectroscopy as well as ligand field and simultaneous pair excitations whose intensities are increased by the spin coupling in the V−O−Mn system.[28] Although on the basis of the structure one might be tempted to view **1** as a V^{IV}═O with only a very weak Mn interaction, such an interaction must be significant as simple V^{IV}═O···V^{IV} head to tail dimers and polymers or mononuclear V^{IV} or Mn^{II} complexes which have similar structural parameters do not display such optical spectra.

Acknowledgment. This work was supported by Grants AI-1157 from the Robert A. Welch Foundation, and SF-93-12 from the Dreyfus Foundation. The NSF-ILI Program Grant USE-9151286 is acknowledged for partial support of the X-ray diffraction facilities at Southwest Texas State University. We also gratefully acknowledge Prof. C. J. O'Connor, University of New Orleans, for the collection of the variable-temperature magnetic data.

Supporting Information Available: Complete list of atomic positions, bond lengths and angles, anisotropic thermal displacement parameters, hydrogen atom coordinates, data collection, and crystal parameters for **1** (8 pages). Ordering information is given on any current masthead page.

IC9615335

(26) Goodenough, J. B. *Magnetism and the Chemical Bond*; Interscience Publishers: New York, 1963.

(27) Hotzelmann, R.; Wieghardt, K.; Floerke, U.; Haupt, H. J.; Weatherburn, D. C.; Bonvoisin, J.; Blondin, G.; Girerd, J. J. *J. Am. Chem. Soc.* **1992**, *114*, 1681.

(28) Schugar, H. J.; Rossman, G. R.; Barraclough, C. G.; Grey, H. B. *J. Am. Chem. Soc.* **1972**, *94*, 2683.